Underwater Localization using Time and Frequency Multiplexing of Circular and Spiral Acoustic Fields

Rúben S. Viegas*, Friedrich Zabel†, António Silva‡ and João Gomes*
*Institute for Systems and Robotics/LARSyS, Instituto Superior Técnico, Universidade de Lisboa, Lisboa, Portugal
†Marsensing Lda, Faro, Portugal
‡CISCA, Universidade do Algarve, Faro, Portugal
Emails: ruben.viegas@tecnico.ulisboa.pt; fredz@marsensing.com; asilva@ualg.pt; jpg@isr.tecnico.ulisboa.pt

2024 Seventh Underwater Communications and Networking Conference (UComms) | 979-8-3315-4251-1/24/$31.00 ©2024 IEEE | DOI: 10.1109/UCOMMS64662.2024.10847977

***Abstract*—The transmission of circular and spiral acoustic fields using spiral beacons offers a promising alternative to traditional underwater localization methods. Existing literature typically employs time multiplexing of these field types. This work introduces a novel approach by implementing both time and frequency multiplexing of circular and spiral fields, specifically transmitting three circular and one spiral field at distinct times and frequencies. The proposed multiplexing methods were evaluated at two different underwater environments: a controlled pool environment and a natural lagoon setting. The localization results demonstrate that the proposed method significantly reduces azimuth variability and confirms its functionality in a lagoon, although with less accuracy compared to the pool test. Overall, time and frequency multiplexing proved to be an effective strategy to enhance current spiral beacon systems and holds potential for advancing new underwater joint communication and localization techniques.**

***Index Terms*—Spiral Source, Underwater Acoustics, Underwater Localization, Signal Processing**

I. Introduction

A Spiral Beacon is a static underwater spiral acoustic source that can be used to perform underwater navigation [1], [2] and SONAR target detection [3]. Spiral acoustic fields offer a promising alternative to traditional methods in underwater applications that, typically, rely on measuring the time of flight (TOF) of the acoustic signal to perform localization, using multiple omnidirectional hydrophones or/and projectors, such as baseline methods [4]–[6] and networking techniques [7]–[9]. The employment of spiral fields stands out for its simplicity, requiring only a single source/hydrophone pair for localization [2], [10].

For correct operation of spiral-field methods, it is necessary to emit a spiral field and a circular field. The spiral field exhibits a linear phase shift concerning the azimuth, while the circular field maintains a constant phase along the azimuth and works as a reference field that nullifies phase changes caused by the environment. The phase difference between the two fields reveals the hydrophone's azimuth. So far, the most common approach is to transmit the circular field followed by the spiral field in the same frequency band [1]–[3], [10]–[12], which is known as time multiplexing.

This work presents an innovative way to perform underwater localization with circular and spiral fields using Time and Frequency Multiplexing. This method is described in Section II. The underwater experiments are described in Section III and the respective results are shown in Section IV. Section V summarizes the main findings and discusses potential extensions for integrated localization and communication applications.

II. Data Model

The data model of the Spiral Beacon system includes the characteristics of the acoustic signals to be transmitted and the methods for processing them after they are received by a single mobile hydrophone.

A. Transmission Side

The developed spiral source prototype, described in [12], has a cylindrical shape with four quadrants, A, B, C, and D. The four quadrants are not acoustically isolated, thus resulting in a transducer with four monopoles that must be driven by four independent signal generators simultaneously. The circular field is created when the input signals for all four quadrants are the same. In contrast, the spiral field requires that the input signals for the four quadrants be in phase quadrature. This makes the piezoceramic vibrate in mode 1 [10] which results in an acoustic signal with a phase that varies linearly with the azimuth. This design has two relevant particularities: the transmission of the circular and spiral fields have resonances at different frequencies ($f_0 = 15.0$ kHz and $f_1 = 22.5$ kHz, respectively), and the circular field has acceptable Transmitting Voltage Response (TVR) at f_1.

Localization using a Spiral Beacon requires the loop transmission of a sequence of signals. In all four quadrants, the proposed transmission sequence has the structure presented in Figure 1: a synchronization signal followed by circular and spiral signals, and another synchronization signal. The circular and spiral signals are upward linear chirps with duration d, bandwidth BW, and center frequency f_0 or f_1. The circular signals (orange signals) are exactly the same in the four quadrants with initial phase of 0°, while in the spiral signals (blue signals) the initial phase is 0°, 90°, 180° and 270°, for quadrants A, B, C, and D, respectively. The signal $x_\alpha(t)$ is the sum of two circular chirps centered at f_0 and f_1, and the signal $x_\beta(t)$ is the sum of a circular chirp centered at f_0 with a spiral chirp centered at f_1. The synchronization signal is a broadband circular signal in the frequency range $[f_{0,s}, f_{1,s}]$ with duration T that is used to estimate the channel and the Doppler factor, and to temporally synchronize received signals. Between the transmission of consecutive signals there is a silence of p seconds for multipath dissipation.

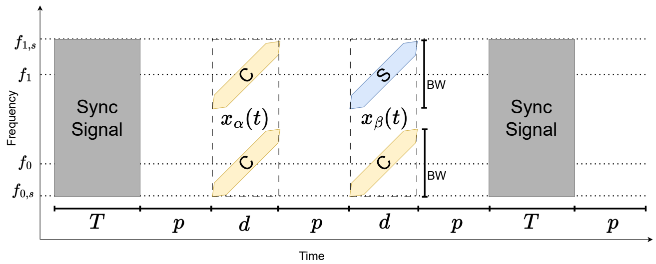

Fig. 1: Structure of the proposed transmission sequence at each quadrant: a synchronization signal followed by circular and spiral signals, and another synchronization signal.

The circular and spiral signals were designed to be transmitted with maximum power, based on the TVR of the aforementioned prototype. The proposed sequence allows for phase differences not only between different signals over time (time multiplexing), but also between different frequencies within the same signal (frequency multiplexing), enabling the comparison of circular and spiral phases simultaneously.

B. Reception Side

Assuming that the Spiral Beacon is static and transmits a known sequence in loop, an underwater system with a single hydrophone can be localized using the received acoustic signals, $y(t)$. Figure 2 shows the signal processing chain. The Doppler Estimation block uses $y(t)$ to estimate the Doppler factor, $\widehat{s}$, and the delay of the direct path, $\widehat{\tau}$. The delay $\widehat{\tau}$ and the sound speed in water c are used to compute the range $\widehat{r}$ between the spiral beacon and the hydrophone. The received signal together with $\widehat{s}$ are used to extract the circular and spiral signals, $y_\alpha(t)$ and $y_\beta(t)$, that are the received versions of $x_\alpha(t)$ and $x_\beta(t)$. Finally, the azimuth angle, $\widehat{\theta}$, is computed using $y_\alpha(t)$ and $y_\beta(t)$.

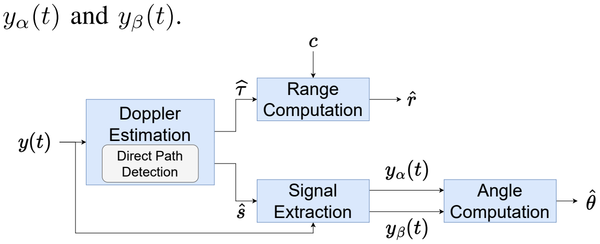

Fig. 2: Signal processing chain: Doppler estimation using direct path detection, range computation, signal extraction and angle computation.

1) Doppler Estimation: This processing step aims to compute the Doppler factor, $\widehat{s}$, using the Scaling Factor Method described in [13]. The average Doppler factor is given by

$$\widehat{s} = \frac{\Delta t}{\Delta t_{\mathrm{s}}} \tag{1}$$

where Δt is the transmission time between the beginning of the first and the beginning of the second synchronization signals, and Δt_{s} is the reception time between the beginning of the first and the beginning of the second synchronization signals. Δt_{s} is computed by subtracting the direct path delays of the second and first synchronization signals, using the direct path detection method. Alternative methods, such as Doppler filter banks, can also be used [14].

The direct path detection method returns the delay of the first path of the Channel Impulse Response (CIR) estimate. The CIR estimate was obtained through cross-correlation between the transmitted and received signals.

The direct path delay of the first synchronization signal, $\widehat{\tau}$, is also used as input for the range computation.

2) Range Computation: In the absence of TX-RX synchronization, the range of the hydrophone relative to the spiral beacon can be computed from a start range measurement, r_0, and by tracking variations in the delay of the first arrival. The range computation N sequences after measuring r_0, without Doppler effect, is given by

$$\widehat{r}_N = r_0 + \sum_{n=1}^{N} c\left(\widehat{\tau}_n - \widehat{\tau}_{n-1} - d_{\mathrm{seq}}\right), \tag{2}$$

where $\widehat{\tau}_n$ is the relative delay obtained at the n^{th} sequence after measuring r_0, and d_{seq} is the duration of the transmitted sequence, including silences. In practice, r_0 must be calibrated so the system starts with the true range. Otherwise, TX-RX synchronization is needed using, e.g., chip-scale atomic clocks.

3) Signal Extraction: In order to compute the azimuth angle $\widehat{\theta}$ based on phase measurements, it is essential to correctly extract the circular and spiral signals taking into account the scaling factor $\widehat{s}$. To compensate for $\widehat{s}$ the received signal is resampled with a polyphase filter, as suggested in [13]. After resampling, it is possible to extract the circular and spiral signals based on the transmission durations.

4) Angle Computation: In its most basic form, the phase difference between spiral and circular fields is computed from spectral measurement at the single central frequency of the two received chirps. In the time multiplexing method both fields occupy the same frequency band, so the measurements have to be spaced in time and are therefore affected by channel variations. In the new frequency multiplexing scheme the spectral measurements for spiral and circular fields are simultaneous on two different frequency bands. An earlier, purely circular, transmission on the same bands provides a baseline for the phase shift introduced by the channel between these frequencies, which should be subtracted out. The rationale is that phase *differences* in the channel response between close bands should vary slower over time than the absolute phase in a single band.

The phase difference for a Time and Frequency Multiplexing sequence is given by

$$\Delta\phi = \mathrm{PD}\left(y_\beta(t), f_1, y_\beta(t), f_0\right) - \mathrm{PD}\left(y_\alpha(t), f_1, y_\alpha(t), f_0\right), \tag{3}$$

where $\mathrm{PD}(\cdot)$ represents the narrowband phase difference operation, given by

$$\mathrm{PD}\left(a(t), f_a, b(t), f_b\right) = \arg\left[\frac{A(f_a)}{B(f_b)}\right], \tag{4}$$

where arg(·) is the complex argument function, and $A(f)$ and $B(f)$ are the Fourier transform values of $a(t)$ and $b(t)$, respectively, at frequency f.

Based only on the Time Multiplexing, the phase difference, using the same sequence, is given by

$$\Delta\phi = \mathrm{PD}\left(y_\alpha(t), f_1, y_\beta(t), f_1\right). \quad (5)$$

Both (3) and (5) were used when analyzing experimental data. The azimuth angle is given by

$$\widehat{\theta} = \Delta\phi - \theta_0, \quad (6)$$

where θ_0 represents an azimuth offset and is a calibration parameter.

III. Underwater Experiments

Two experiments were carried out to evaluate the performance of the proposed system: one at a controlled pool environment and the other at a natural lagoon setting. Table I shows the parameters that were used for these experiments. Up-down chirps were used as synchronization signals with the aim of studying alternative methods for estimating the Doppler factor, but details are deferred to forthcoming work.

TABLE I: Parameters of the used sequences in Pool and Lagoon experiments.

Parameter	T (ms)	d (ms)	p (ms)	$f_{0,s}$ (kHz)	$f_{1,s}$ (kHz)	BW (Hz)
Pool	20	2	100	10	25	500
Lagoon	151	2	200	10	25	500

A. Pool Experiment

The experiment was carried out in a 16 by 16 m pool with 4.3 m depth. The experiment setup consists of placing the spiral beacon system at the bottom of the pool so that it remains as static as possible. The Spiral Source was placed at 1.37 m from the bottom. In this setup, a hydrophone RESON TC4033 was placed 2.08 m from the surface, attached to a separate floating structure for mobility. The hydrophone's true localization was obtained by recording its position from the top of the pool. For more details on the experimental setup, refer to [12].

B. Lagoon Experiment

The experiment was carried out in Ria Formosa Lagoon, Faro, Portugal. The spiral source and the underwater container were placed at the bottom (approx. 4 m depth) and a Marsensing SR-1 hydrophone was attached to a kayak equipped with a Handheld GPS Navigator. The kayak navigated through the lagoon and the GPS coordinates were acquired together with the acoustic signals from the hydrophone, at approx. 2 m from the surface. Figure 3 shows the spiral source and the underwater container near the anchorage site.

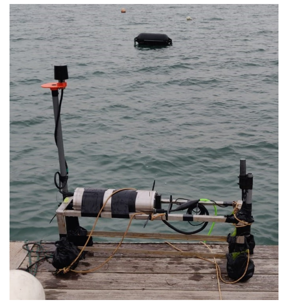

Fig. 3: Spiral source and underwater container near the anchorage site at the Lagoon.

IV. Localization Results and Discussion

The localization of the mobile hydrophone in both experiments was computed based on the described methods, considering r_0 as the ground truth range at the beginning of the experiment, and θ_0 as an *a posteriori* value that best fits the azimuth data, since the underwater orientation of the Spiral Beacon was unknown. In both experiments the signals were split due to recording problems in some sections of the path.

Figures 4a and 4b show the localization comparison between the ground truth (dashed curves) and the Spiral Beacon method in the two experiments: Pool, and Lagoon, respectively. Both figures show the azimuth angle estimate using the Time Multiplexing (red) and the Time and Frequency Multiplexing (green), and the range estimate (solid black). The azimuth angle estimate curves presented are the angle after filtering with a phase-wrapped moving average filter with a window size of 13 and 101 samples for the Pool and Lagoon experiment, respectively. The shaded uncertainty region corresponds to the phase-wrapped standard deviation of the phase-wrapped moving average samples. Although the average angles of the two acoustic methods are similar, the standard deviation of time and frequency multiplexing is relatively lower, making this method more accurate for estimating the azimuth angle. Comparing the results of the two experiments, it is possible to observe that the location with the Spiral Beacon is dependent on the environment, as the azimuth mean error and variability are larger in the Lagoon experiment, thus resulting in worse performance. Furthermore, in the Lagoon case, a greater number of samples is needed to obtain an acceptable average value.

Figures 5a and 5b show the 2D tracks of Figures 4a and 4b, namely, the ground truth localization (black) versus the Spiral Beacon localization (yellow), using Time and Frequency Multiplexing. It is possible to observe that the acoustic localization error is higher in the Lagoon experiment, probably due to the low SNR and the high interference of the acoustic channel.

The overall results show that Time and Frequency Multiplexing is a method that performs better than the standard method (Time Multiplexing), but still presents limitations in Lagoon environments where the channel's multipath varies rapidly over time due to the shallow water and the surface waves.

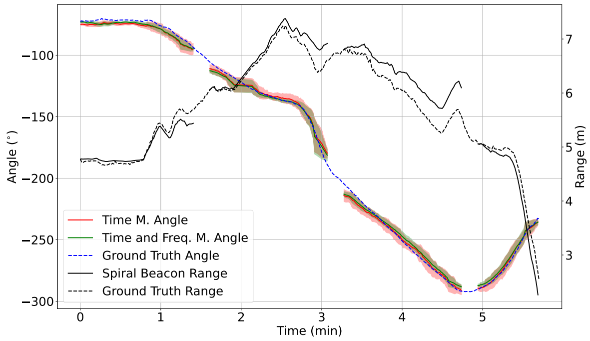

(a)

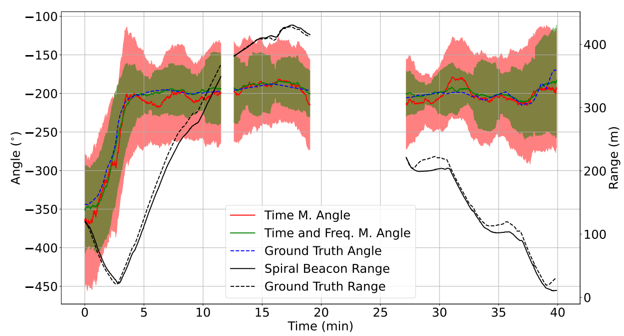

(b)

Fig. 4: Localization comparison between the ground truth (dashed curves) and the Spiral Beacon method in the two experiments: (a) Pool, and (b) Lagoon. Both figures show the azimuth angle estimate using Time Multiplexing (red) and Time and Frequency Multiplexing (green), as well as the range estimate (solid black).

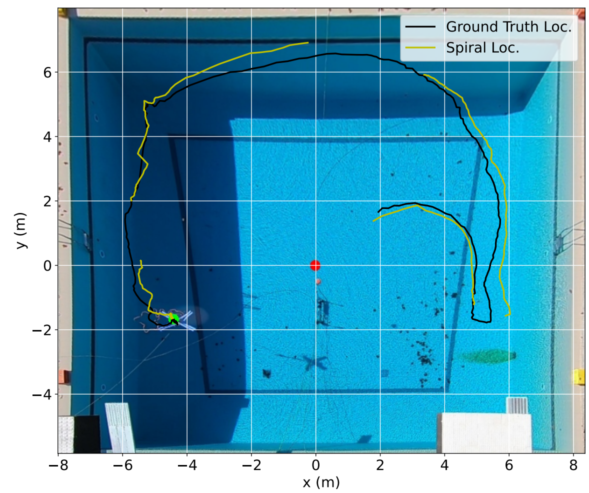

(a)

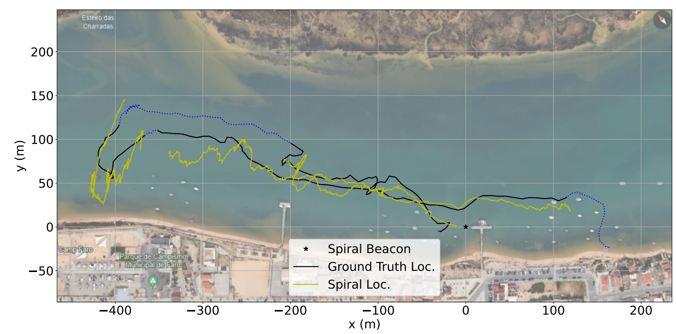

(b)

Fig. 5: 2D Representation of the ground truth localization (black) versus the Spiral Beacon localization (yellow) using the Time and Frequency Multiplexing in the two experiments: (a) Pool, and (b) Lagoon.

V. Conclusion

Underwater Localization using spiral fields is an alternative to traditional acoustic methods that only requires a single source/hydrophone pair to operate. This work presents a new way to operate the circular and spiral fields using Time and Frequency Multiplexing. This new method showed less localization variability compared to the standard method (Time Multiplexing). Furthermore, the spiral source design with a single piezoelectric ceramic was tested for the first time in an uncontrolled underwater environment. Even in a shallow water channel with a maximum depth of 4 meters and with vertical and horizontal motion of the hydrophone, it was possible to roughly localize it. That was possible due to the short signal duration, which overcomes the multipath and channel variability. The use of spiral fields still presents some limitations, namely, the variability of azimuth estimation, which is related to close multipath arrivals of the acoustic channel. Future processing must detect the direct path and isolate it so that there is no interference for any duration of the signal.

Recently, there has been much interest on the topic of integrated sensing and communications (ISAC), which advocates the dual-use of communication waveforms (e.g., in 5G/6G cellular networks) for other purposes, such as localization or bistatic sonar/radar. The orthogonal chirp-division multiplexing (OCDM) modulation format seems to be a natural candidate for dual use in sonar, and has indeed been examined recently for such use in the context of underwater communication [15]. Integration with OCDM for joint data transmission and single-receiver localization using a spiral source is also envisaged as a future research direction for this work.

VI. Acknowledgement

We would like to thank the City Council of Loulé, namely to its President Vítor Aleixo and Mr. Pedro Gema, for providing the use of the Loulé City Pools to carry out the acoustic experiments.

This work was supported by LARSyS FCT funding (DOI: 10.54499/LA/P/0083/2020, 10.54499/UIDP/50009/2020, and 10.54499/UIDB/50009/2020).

Rúben S. Viegas is supported by a Portuguese Foundation for Science and Technology grant (DOI: 10.54499/2023.03744.BD).

References

[1] B. R. Dzikowicz, B. T. Hefner, and R. A. Leasko, "Underwater acoustic navigation using a beacon with a spiral wave front," *IEEE Journal of Oceanic Engineering*, vol. 40, no. 1, pp. 177–186, 1 2015.

[2] B. R. Dzikowicz, J. Y. Yoritomo, J. T. Heddings, B. T. Hefner, D. A. Brown, and C. L. Bachand, "Demonstration of spiral wavefront navigation on an unmanned underwater vehicle," *IEEE Journal of Oceanic Engineering*, pp. 1–10, 2023.

[3] B. R. Dzikowicz, J. F. Tressler, and D. A. Brown, "Demonstration of spiral wave front sonar for active localization," *The Journal of the Acoustical Society of America*, vol. 146, no. 6, pp. 4821–4830, 12 2019.

[4] A. Munafo, J. Sliwka, G. Ferri, A. Vermeij, R. Goldhahn, K. LePage, J. Alves, and J. Potter, "Enhancing AUV localization using underwater acoustic sensor networks: Results in long baseline navigation from the COLLAB13 sea trial," in *2014 Oceans - St. John's*. IEEE, 9 2014.

[5] C. Militello and S. R. Buenafuente, "An exact noniterative linear method for locating sources based on measuring receiver arrival times," *The Journal of the Acoustical Society of America*, vol. 121, no. 6, p. 3595, 2007.

[6] N. R. Rypkema, E. M. Fischel, and H. Schmidt, "Closed-loop single-beacon passive acoustic navigation for low-cost autonomous underwater vehicles," in *2018 IEEE/RSJ International Conference on Intelligent Robots and Systems (IROS)*. IEEE, 10 2018.

[7] L. Paull, S. Saeedi, M. Seto, and H. Li, "AUV navigation and localization: A review," *IEEE Journal of Oceanic Engineering*, vol. 39, no. 1, pp. 131–149, 2014.

[8] X. Su, I. Ullah, X. Liu, and D. Choi, "A review of underwater localization techniques, algorithms, and challenges," *Journal of Sensors*, vol. 2020, pp. 1–24, 2020.

[9] S. Sun, T. Liu, Y. Wang, G. Zhang, K. Liu, and Y. Wang, "High-rate underwater acoustic localization based on the decision tree," *IEEE Transactions on Geoscience and Remote Sensing*, vol. 60, pp. 1–12, 2022.

[10] R. Viegas, F. Zabel, and A. J. Silva, "In-lab demonstration of an underwater acoustic spiral source," *Sensors*, vol. 23, no. 10, p. 4931, May 2023.

[11] R. Viegas, F. Zabel, and A. J. Silva, "Underwater acoustic spiral source: pool tests and calibration," in *OCEANS 2023 - Limerick*. IEEE, Jun. 2023.

[12] R. S. Viegas, F. Zabel, J. Gomes, and A. Silva, "Spiral beacon calibration and experiments for underwater localization," in *OCEANS 2024 - Singapore*, 2024, Available here.

[13] B. Li, S. Zhou, M. Stojanovic, L. Freitag, and P. Willett, "Multicarrier communication over underwater acoustic channels with nonuniform doppler shifts," *IEEE Journal of Oceanic Engineering*, vol. 33, no. 2, p. 198–209, Apr. 2008.

[14] D. K. Barton, *Radar System Analysis and Modeling*, 2nd ed. Artech House, 2005.

[15] J. Wang, Q. Tao, G. Han, X. Fu, and Q. Wang, "Orthogonal chirp division multiplexing based on dictionary theory for integrated sonar and communication system," *IEEE Communications Letters*, p. 1–1, 2024.